Climate Dynamics
https://doi.org/10.1007/s00382-023-06848-x

Relationships among Arctic warming, sea-ice loss, stability, lapse rate feedback, and Arctic amplification

Aiguo Dai[1] · **Matthew T. Jenkins**[1]

Received: 3 February 2023 / Accepted: 29 May 2023

Abstract
The Arctic warms much faster than other places under increasing greenhouse gases, a phenomenon known as Arctic amplification (AA). Arctic positive lapse-rate feedback (LRF) and oceanic heating induced by sea-ice loss have been considered as major causes of Arctic warming and AA, and Arctic high atmospheric stability has been considered as a key factor for the occurrence of the bottom-heavy warming profile and thus positive LRF in the Arctic. Here we analyze model simulations with and without large AA and sea-ice loss and long-term changes in ERA5 reanalysis data to examine the relationships among Arctic sea-ice loss, stability, LRF, Arctic warming, and AA. Results show that the Arctic bottom-heavy warming profile and the resultant positive LRF are produced primarily by increased oceanic heating of the air due to sea-ice loss in Arctic winter, rather than high atmospheric stability. Without the oceanic heating induced by sea-ice loss, most Arctic climate feedbacks weaken greatly, and all other processes can only produce slightly enhanced surface warming and thus weak positive LRF under stable Arctic air. A non-convective Arctic environment allows the oceanic heating to warm near-surface air more than the upper levels, resulting in large positive LRF that roughly doubles the surface warming compared with the case without the LRF. We conclude that enhanced cold-season oceanic heating due to sea-ice loss is the primary cause of Arctic large positive LRF, which in turn allows the surface heating to produce more Arctic warming and large AA.

Keywords Arctic warming · Sea-ice loss · Ocean heat release · Lapse rate feedback · Stability · Arctic amplification

1 Introduction

Arctic surface temperature warms faster than the global mean in observations and climate models under rising greenhouse gases – a phenomenon known as Arctic amplification (AA; Serreze et al. 2009; Barnes and Polvani 2015; Dai et al. 2019; Hahn et al. 2021; Previdi et al. 2021; Taylor et al. 2022). Previous studies cite increased poleward energy transport (Cai 2005; Soldatenko 2021), enhanced downward longwave (LW) radiation (Burt et al. 2016; Gong et al. 2017), and positive climate feedbacks (Bintanja et al. 2011; Pithan and Mauritsen 2014; Goosse et al. 2018; Stuecker et al. 2018; Previdi et al. 2020) as the primary causes of AA. However, many of these processes depend on Arctic warming itself, entangling the cause and effect of AA in a fully coupled system. Further, they cannot fully explain the spatial patterns and seasonality of AA, which occurs mainly over areas with large sea-ice loss during the cold season (Dai et al. 2019). Therefore, the key mechanisms underlying AA are still debated (Previdi et al. 2021; Taylor et al. 2022).

Early studies (Serreze and Francis 2006; Serreze et al. 2009) linked AA to summer sea-ice loss. More recent studies suggest that enhanced oceanic heating of the atmosphere from October-March due to sea-ice loss during the cold season produces AA (Deser et al. 2010; Kumar et al. 2010; Screen and Simmonds 2010a; Boeke and Taylor 2018; Dai et al. 2019; Chung et al. 2021; Jenkins & Dai 2021). During the warm season, sea-ice melting exposes water surfaces that absorb and store solar radiation in the upper ocean. As air temperatures decrease in autumn and winter, open water surfaces release energy to heat the air through upward LW radiation, sensible and latent heat fluxes. Sea-ice loss increases warm-season oceanic absorption of solar radiation and cold-season oceanic heating of Arctic air, leading to

✉ Aiguo Dai
adai@albany.edu

[1] Department of Atmospheric and Environmental Sciences, University at Albany, SUNY, Albany, NY, USA

large AA in the cold season (Screen and Simmonds 2010b; Boeke and Taylor 2018; Dai et al. 2019). This positive sea ice-induced feedback (named *sea-ice feedback* here, illustrated in Fig. 1) differs from the conventional ice-albedo feedback, which does not include the warm-season oceanic storing of the absorbed solar radiation and cold-season release of oceanic heat due to the reduced *insulation* effect of the retreating sea-ice layer. Also note that the increased cold-season ocean heat release does not collocate exactly with the enhanced warm-season shortwave absorption as the cold-season and warm-season sea-ice loss occurs over different regions (Dai et al. 2019). This suggests that the increased cold-season heat release does not come directly from the increased warm-season absorption of solar radiation, although the latter appears to be an important energy source of the former as we show below. Dai et al. (2019) further showed that no large AA could occur without sea-ice loss. Previdi et al. (2020) showed that noticeable AA started to appear a few months after the CO_2 quadrupling (apparently on January 1st) as Arctic sea-ice loss becomes evident, even though they stated that Arctic amplification occurs before significant sea-ice loss. Thus, enhanced oceanic heating from sea-ice loss seems to be necessary for large AA to occur through the sea-ice feedback (Dai et al. 2019; Chung et al. 2021).

Arctic sea-ice loss is caused by surface heating or warming; thus, any process that enhances surface warming may contribute to sea-ice loss and thus AA indirectly. These include the positive water vapor feedback, cold-season positive cloud feedback, and Arctic positive lapse feedback (LRF) that amplify Arctic warming and thus enhance sea-ice loss, thereby contributing to AA. This indirect effect through sea-ice loss differs from the direct warming effect by the feedbacks. For example, the water vapor feedback is stronger in the tropics than the Arctic; thus, its direct warming effect contributes negatively to AA (Pithan and Mauritsen 2014). However, this warming effect in the Arctic enhances sea-ice loss, thereby indirectly contributing

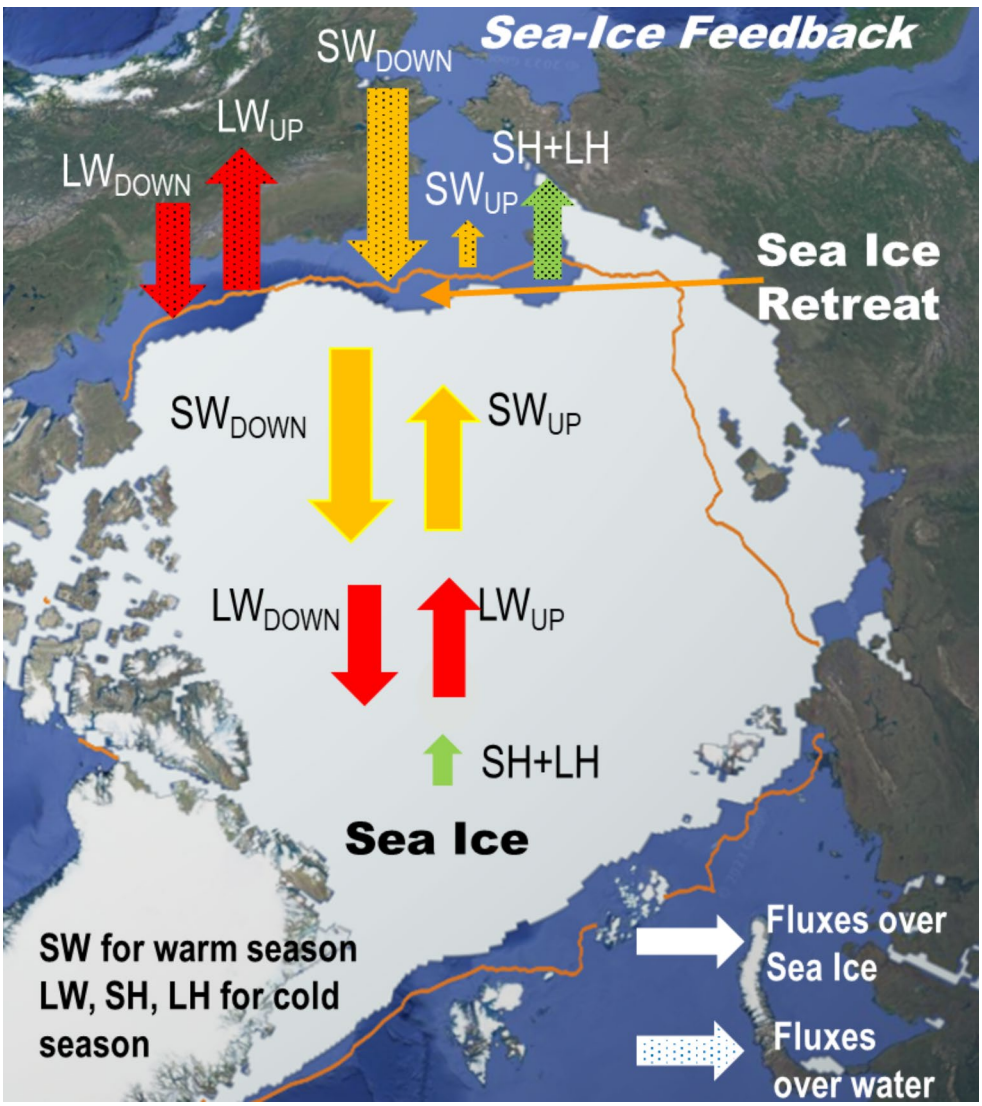

Fig. 1 A schematic illustrating the positive*sea-ice feedback*that is largely responsible for Arctic amplification (AA). Sea-ice retreat exposes dark water surfaces that absorb more solar radiation (SW) during the warm season (the ice-albedo feedback) and release more upward longwave radiation (LW), sensible (SH) and latent heat (LH) fluxes (the reduced insulation effect) to heat the frigid Arctic air in the cold season, thus causing more warming and sea-ice loss. The increased warm-season absorption of solar radiation by the ocean does not cause significant surface warming during the warm season and it only accounts for a fraction of the local increased cold-season heat release over areas with large sea-ice loss. The *cold-season* sea-ice loss and its resultant oceanic heat release play a crucial role in causing enhanced surface warming (i.e., AA) and large positive lapse-rate feedback. The *sea-ice feedback* occurs mainly around the ice margins and it includes the warm-season sea-ice albedo feedback, the storing of the absorbed SW radiation by the ocean, and the cold-season release of oceanic heat due to the reduced insulation effect of the retreating sea ice; thus it differs from the conventional ice-albedo feedback

to Arctic warming and AA through the sea-ice feedback described above. More clouds are found to form over open water surfaces in autumn in the Arctic (Kay and Gettelman 2009) and the largest cloud increases are seen over areas with large sea-ice loss (Jenkins et al. 2023), which can lead to positive cloud feedback during the cold season (Jenkins & Dai 2021, 2022) that can enhance Arctic warming and sea-ice loss. The northern high latitudes experience greater warming near the surface than the mid-to-upper troposphere under increased GHGs during the cold season (Screen and Simmonds 2010a; Dai and Song 2020; Taylor et al. 2022). This bottom-heavy warming profile reduces the top-of-the-atmosphere (TOA) LW cooling, thus allowing the surface to warm more under a given GHG increase (Bintanja et al. 2011; Hahn et al. 2021), leading to a positive LRF. In contrast, tropical convection transports energy and moisture from the lower to mid-upper troposphere, where latent heating from condensation enhances warming aloft (Dai et al. 2001; Miyawaki et al. 2020; Wang and Huang 2021). This leads to an upper-heavy warming profile that increases outgoing LW radiation and thus weakens the GHG-induced warming; thus, the LRF produces slight cooling in low latitudes but strong warming in northern high-latitudes (Pithan and Mauritsen 2014). Because of this, Arctic positive LRF has been considered as a major contributor to AA.

However, in a fully coupled system, near-surface and lower-tropospheric air temperatures strongly influence downward and upward LW radiation, LRF, and atmospheric meridional energy transport (Jenkins & Dai 2021), making it difficult to separate the cause and effect between Arctic warming (or AA) and these individual processes, including LRF. For example, the calculated LRF strongly depends on surface air temperature (SAT) change, which can be produced by other factors besides LRF, such as heating from the ocean. Thus, such calculated LRF may include contributions or effects from other processes that can enhance surface warming relative to upper levels. In other words, the large positive LRF in the Arctic may be considered partly as a result of the enhanced Arctic surface warming caused by oceanic heating and other processes, rather than a pure contributor to Arctic warming. On the other hand, the existence of the positive LRF under a bottom-heavy warming profile caused by the surface heating would allow the heating to produce larger surface warming than the case without the LRF. This illustrates the complex cause-and-effect relationship between Arctic LRF and Arctic warming or AA.

Early studies attributed the Arctic bottom-heavy warming profile to Arctic high atmospheric stability, which was thought to confine GHG-induced warming near the surface (e.g., Manabe and Wetherald 1975; Hansen et al. 1984). However, recent studies show that sea-ice loss, ocean-to-atmosphere energy fluxes and the resultant surface warming, rather than the degree of atmospheric stability, largely shape Arctic LRF under a non-convective environment (Feldl et al. 2020; Boeke et al. 2021; Jenkins & Dai 2021). Nevertheless, the role of stability and sea-ice loss is still debated. For example, Feldl et al. (2020) considered sea-ice loss as the primary cause of Arctic LRF through surface albedo feedback, while Boeke et al. (2021) proposed a multiple-process perspective where the mechanisms responsible for the nonuniform warming profile determine LRF but they did not investigate these mechanisms. Both studies derived their conclusions mainly based on spatial and inter-model relationships among LRF, stability, sea-ice loss, and surface warming in fully coupled CMIP5 models, in which it is difficult to disentangle the cause and effect between LRF and Arctic warming. It should be emphasized that the conventional ice-albedo feedback works only in Arctic warm season when Arctic LRF is weak (Jenkins & Dai 2021), and it does not include the reduced insulation effect of the retreating cold-season sea ice that is largely responsible for AA (Dai et al. 2019). Jenkins & Dai (2021), who did not examine atmospheric stability, suggested that Arctic positive LRF is likely a result, rather than a cause, of AA based on brief analyses of their spatial patterns and seasonality. However, a thorough analysis of the relationship among Arctic warming, sea-ice loss, stability, and LRF is still lacking. In particular, the processes or mechanisms that are largely responsible for the occurrence of Arctic positive LRF is unclear. Further, the contribution of Arctic LRF to Arctic surface warming (and thus AA) has not been fully quantified. Motivated by these outstanding issues, here we analyze model simulations and ERA5 data to examine the relationship between winter Arctic warming and LRF, and their associations with Arctic stability, sea-ice loss, and oceanic heating. We provide new evidence to show that the Arctic bottom-heavy warming profile and the associated positive LRF are largely a result of the enhanced oceanic heating produced by sea-ice loss under a non-convective environment, and that the existence of the positive LRF in turn allows the oceanic heating to warm Arctic surface air twice as faster as the case without the LRF. Our results further confirm the crucial role of sea-ice loss in causing AA and help disentangle the complex relationships among Arctic warming, sea-ice loss, oceanic heat release, bottom-heavy warming profile, LRF, and stability.

2 Data and method

2.1 Model simulations and reanalysis data

We analyzed a 150-year preindustrial control run (CTL) with atmospheric CO_2 fixed at 284.7ppmv, a 1%CO_2 run

and a FixedIce run (both with 1%/year CO_2 increase for 235 years) with the Community Earth System Model version 1 (CESM1; Hurrell et al. 2013) on 2.5° longitude × ~2.0° latitude grids and 26 vertical levels for the atmosphere, and ~1.0° longitude × 0.5° latitude grids for sea ice and oceans. These simulations were used and described in Dai et al. (2019), Dai and Song (2020), Jenkins & Dai (2021), and Dai (2022). We focus on winter (December-January-February or DJF) when AA and Arctic positive LRF are most pronounced (Dai et al. 2019; Jenkins & Dai 2021) for the analyzed changes averaged over years 131–150 (around the time of quadrupling of preindustrial CO_2) relative to CTL climatology, when the CO_2-forced changes dominate over internal variations in the 20-year averages. The FixedIce run is the same as the 1%CO_2 run except that fixed sea-ice cover (SIC) derived from the CTL climatology is used north of 30ºN only in the coupler of the model for determining the ice and water fractions used as the weighting factors for calculating oceanic grid-box mean values of all surface exchange fluxes. In FixedIce, sea ice and all other ice-related, atmospheric, and oceanic processes are allowed to evolve dynamically as in the standard CESM1, but the altered fluxes from the coupler affect the internal sea-ice evolution, resulting in smaller sea-ice loss and Arctic warming. The atmosphere and ocean do not "see" any changes or variations (besides the mean seasonal cycle) in SIC in FixedIce, even though its internal SIC varies and decreases slightly. The use of the CTL SIC in the coupler does not violate any physical laws or produce any abrupt or unrealistic changes (Deng and Dai 2022).

For comparison, we also analyzed the long-term changes between two 30-year periods (i.e., 1990–2019 minus 1950–1979) in Arctic SIC, air temperature, and other fields using the ECMWF Reanalysis v5 (ERA5, Hersbach et al. 2020). ERA5 is the newest and likely most advanced atmospheric reanalysis. It used observation-based analysis data for sea surface temperatures (SST) and SIC as the lower boundary conditions (Hirahara et al. 2016) and assimilated available satellite, radiosonde and aircraft observations of the atmosphere and surface pressure, air temperature and humidity observations over the Arctic and other regions (Lawrence et al. 2019). Thus, ERA5 has made use of many observations (including those for SIC) over the Arctic in generating its output. Recent evaluations (Graham et al. 2019; Wang et al. 2019; Yeo et al. 2022) showed overall good performance over the Arctic by ERA5, including its SAT and SIC variations and changes (Dai and Deng 2021). ERA5 also simulates Arctic downward and net LW radiative fluxes well for both winter and summer (Graham et al. 2019). Nevertheless, some systematic biases have been noticed in ERA5 data for Arctic SAT and SIC, especially around the marginal ice zones likely due to insufficient resolution of the SIC data assimilated (Wang et al. 2019; Renfrew et al. 2021). Other known issues of ERA5 include some deficiencies in its representation of surface energy fluxes especially over regions with sea-ice loss (Graham et al. 2019) and biases in cloud properties (too many clouds over sea ice with too little seasonal variation; Yeo et al. 2022). The ERA5 30-year averaged data include externally-forced changes and internally-generated multidecadal variations, although the former likely dominates for Arctic averages since the long-term warming trend is a robust signal over the Arctic (England et al. 2021). Because of the various biases, ERA5 should not be considered as the truth for the real world; nevertheless, it is much more representative of the real world than any model simulation.

2.2 Lapse rate feedback calculations

As the surface and troposphere warm, the Earth emits more LW radiation to space, thus creating a negative temperature feedback (TF), which is often partitioned into two components: a LW cooling under a hypothetical vertically-uniform warming profile (the Planck feedback or PLF) and a residual component due to a vertically nonuniform warming profile (the LRF). Using the TOA (or tropopause) radiative flux as the measure of the forcing created by these feedbacks, this partitioning can be expressed locally as

$$R_T = \int_{pTOA}^{p_o} K_T(p) * \Delta T_a(p)\, dp = \int_{pTOA}^{p_o} K_T(p) * [\Delta T_c + (\Delta T_a(p) - \Delta T_c)]\, dp$$

$$= \int_{pTOA}^{p_o} K_T(p) * \Delta T_c dp + \int_{pTOA}^{p_o} K_T(p) * (\Delta T_a(p) - \Delta T_c)\, dp = R_{PL} + R_{LR} \quad (1)$$

where p_o and p_{TOA} are the surface and tropopause pressure; ΔR_T, ΔR_{PL}, and ΔR_{LR} are the TOA forcing (positive downward) due to the total TF, PLF and LRF, respectively; $K_T(p)$ (in W m^{-2} K^{-1} hPa^{-1}) is the air temperature radiative kernel estimated by perturbing the temperature of a layer centered at level p by 1 K while keeping all other variables fixed to estimate the TOA flux change (Soden et al. 2008; Jenkins & Dai 2021, 2022); $\Delta T_a(p)$ is the temperature change at level p; and ΔT_c represents a hypothetical uniform warming profile. As in Jenkins and Dai (2022), here we used the $K_T(p)$ derived based on ERA-Interim reanalysis (Huang et al. 2017) for estimating the feedbacks in ERA5, and the $K_T(p)$ from Pendergrass et al. (2018) for the CESM1 feedbacks as in Jenkins & Dai (2021). The estimated TOA forcing from the temperature feedbacks is insensitive to the choice of the kernels (Jenkins and Dai 2022). The TF-induced ΔR_T and PLF-induced ΔR_{PL} will always be negative since any warming increases outgoing LW radiation. However, the sign and magnitude of the nonuniform warming-induced ΔR_{LR}

depends on the choice of ΔT_c. In most studies, ΔT_c is set to near-surface warming, producing a positive LRF in the Arctic and a negative LRF in the tropics (Pithan and Mauritsen 2014). To illustrate the impact of this choice, here we also calculated the ΔR_{LR} and the corresponding ΔR_{PL} for a case where ΔT_c is set to the warming in the upper troposphere (i.e., at 313 hPa). The purpose of this exercise is to show that the sign and magnitude of the estimated TOA LW forcing resulting from the nonuniform warming depend on the choice of the hypothetical uniform warming profile (i.e., ΔT_c).

2.3 Potential warming contributions

To compare the *potential* contributions by each feedback to Arctic and global surface warming, we followed the method of Pithan and Mauritsen (2014) to calculate the *potential* warming contribution (ΔT_{sp}) by a given climate feedback: $\Delta T_{sp} = -\frac{R}{\bar{\lambda}_{PL}}$, where ΔR is the TOA radiative flux perturbation caused by the climate feedback and $\bar{\lambda}_{PL}$ is the global-mean Planck feedback parameter. In this calculation, it is implicitly assumed that the TOA flux anomaly causes an equilibrium uniform warming (i.e., LRF=0) so that the increased longwave radiative cooling through the Planck feedback would balance the TOA flux. Clearly, this does not apply to transient warming, which is influenced by many other factors, such as how much of the TOA flux change is used to raise the surface temperature. For example, the ΔR caused by Arctic surface albedo feedback may be used to melt sea ice (i.e., converted into latent energy) or be absorbed by the upper ocean (with small temperature increases), rather than being used to raise surface temperature. Thus, one should not consider the estimated ΔT_{sp} as a real contribution to transient surface warming; it only represents a *potential* warming or cooling contribution after reaching a new equilibrium state under the assumption of LRF=0 for comparison purposes. The only exception is for the TF, PLF and LRF; in which cases, the TOA fluxes are indeed based on the surface temperature changes as shown in Eq. (1) and thus the estimated ΔT_{sp} does represent a contribution to the surface temperature change. Nevertheless, such potential warming (or cooling) amounts have been widely used for comparing the relatively strength of the feedbacks over the Arctic and other regions (e.g., Pithan and Mauritsen 2014; Stuecker et al. 2018; Feldl et al. 2020; Previdi et al. 2020; Hahn et al. 2021), so that their different contributions (to regional energy balance, which may not be the same as to regional surface warming) can be compared quantitatively.

Similarly, we also calculated a surface warming amount ΔT_{sc} that would balance the ΔR_T through the Planck feedback only in Eq. (1), i.e., through a vertically uniform warming amount of ΔT_{sc}, which represents a hypothetical warming amount without the LRF that would result in the same TOA longwave radiative cooling as in Eq. (1). The difference between the ΔT_c from the model simulation (and used in Eq. 1) and ΔT_{sc} represents the warming contribution from the LRF in the model simulation. This provides us a method to quantify the warming contribution by the LRF feedback.

3 Results

Figure 2a shows that Arctic winter warming is much larger near the surface than aloft in the CESM1 1%CO_2 run, while this warming difference is much weaker in FixedIce, despite that they started from the same atmospheric stability, which is measured using the maximum temperature inversion between 929 hPa and the surface (black line in Figs. 2a and 3). Further, in the 1%CO_2 run, the surface warming enhancement is larger over areas with significant ($\geq$15%) sea-ice loss than over areas with little (<15%) sea-ice loss, whereas the inversion is the opposite, i.e., weaker over areas with significant sea-ice loss than over areas with little sea-ice loss (Fig. 2b). Such a relationship is also seen in ERA5 long-term changes from 1950–1979 to 1990–2019 (Fig. 2d), which show stronger enhancement of surface warming over areas with significant sea-ice loss than over areas with little sea-ice loss, whereas the inversion is the opposite. Thus, stronger stratification does not lead to stronger bottom-heavy warming or stronger positive LRF, which is consistent with Boeke et al. (2021), who showed that Arctic LRF does not depend on the degree of stability in CMIP5 models. Due to advection, the enhanced surface warming will spread out to nearby areas as noticed previously (Serreze et al. 2009); thus, part of the warming enhancement over areas with little sea-ice loss in the 1%CO_2 run likely comes from the strong warming over areas with significant sea-ice loss (Fig. 3a). Such a "contamination" is absent in FixedIce, as its warming is relatively uniform horizontally (Fig. 3c). Thus, the warming profile from FixedIce (Fig. 2a) provides a cleaner representation of the impact of atmospheric stability on the CO_2-induced warming under the condition without increased oceanic heating due to sea-ice loss.

The enhanced surface warming results in a strong positive LRF in the 1%CO_2 run, while the LRF is only weakly positive in FixedIce (red and blue bars in Fig. 2c). Because the only difference between these two runs is that the effect of sea-ice loss on surface fluxes is allowed in the 1% CO_2 run but absent in FixedIce, we can conclude that the strong Arctic positive LRF is a result of the sea-ice loss through its impact on surface fluxes, which is mainly through increased oceanic heat release over newly exposed water surfaces as

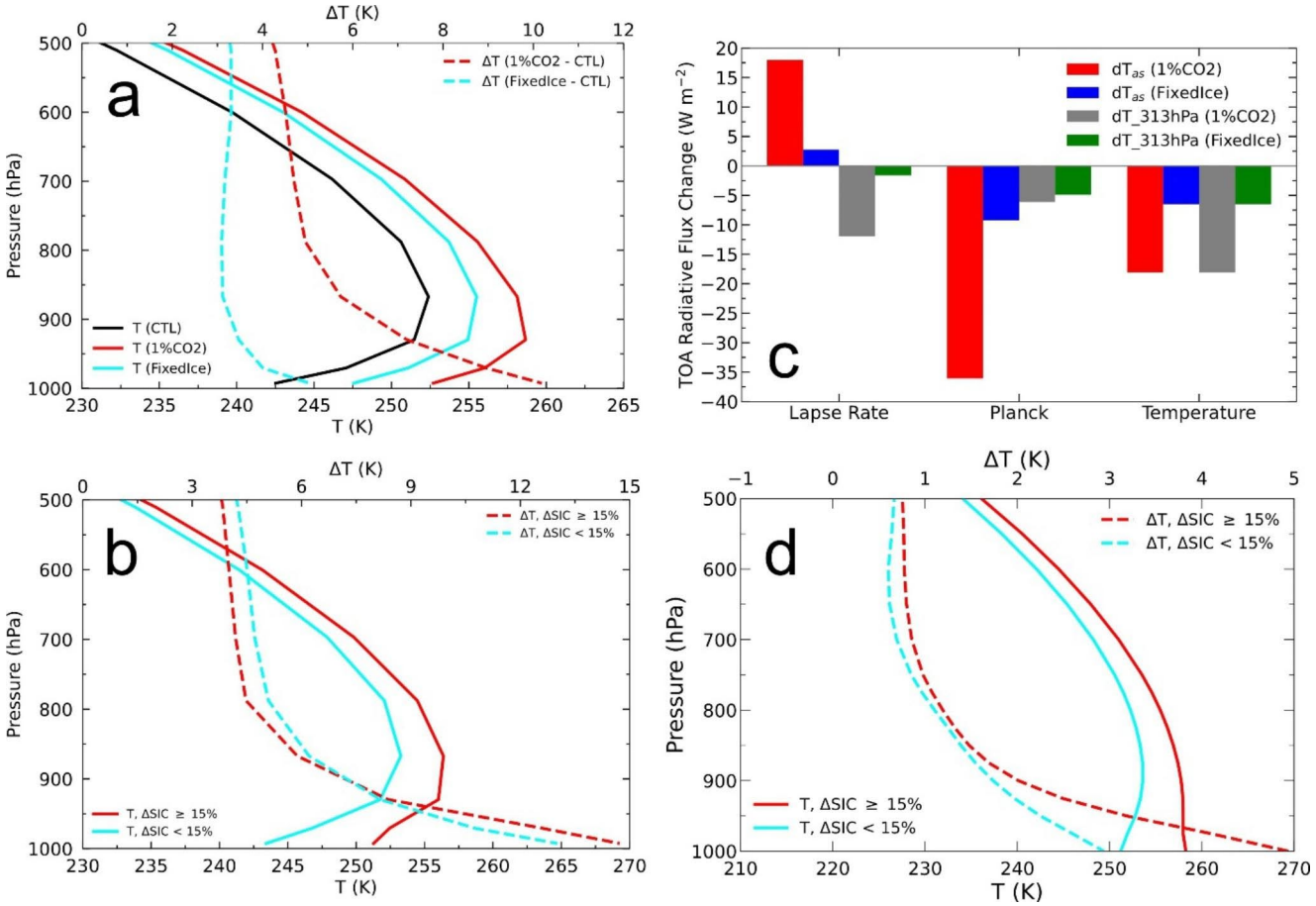

Fig. 2 (**a**) Arctic (67°-90°N) mean DJF temperature profiles (bottom x-axis) for years 1–80 of the CESM1 CTL run (black) and years 131–150 of the CESM1 1%CO_2 (red solid) and FixedIce (cyan solid) runs, and their changes (top x-axis, dashed lines). (**b**) Similar to (**a**) but for the initial profiles from CTL (solid) and their changes (dashed) averaged over oceanic areas with sea-ice loss greater than or equal to 15% (red) or less than 15% (cyan) in the 1%CO_2 run. (**c**) Arctic mean DJF TOA flux changes (positive downward) for years 131–150 relative to the CTL climatology due to the lapse rate, Planck and total temperature feedbacks for the two cases using surface warming (denoted as dT_{as}, red and blue bars) or atmospheric warming at 313 hPa (denoted as dT_313hPa, gray and green bars) in the Planck feedback calculation from the 1%CO_2 run (red and gray bars) and FixedIce run (blue and green bars). (**d**) Similar to (**b**) but for ERA5 DJF temperature profiles (bottom x-axis, solid) averaged over years 1950–1979 and their changes from 1950–1979 to 1990–2019 (top x-axis, dashed) averaged over oceanic areas with significant (≥ 15%, red) or little (< 15%, cyan) sea-ice loss from 1950–1979 to 1990–2019. Land surfaces are excluded from all averages in (**a-d**). Inclusion of land does not qualitatively change the results

we show below. Further, Fig. 2c shows that the ΔR_{LR} due to the nonuniform warming would become negative while the ΔR_{PL} would have a smaller negative value if we set the hypothetical uniform warming amount ΔT_c to the warming amount in the upper troposphere at 313 hPa, even though the net temperature feedback is the same for both cases. This demonstrates that the sign and magnitude of the TOA radiative forcing due to the nonuniform warming depends on how one chooses the hypothetic uniform warming profile used to calculate the Planck feedback.

In both the 1%CO_2 and FixedIce runs, surface warming and LRF are only weakly correlated spatially with the initial stability (r = 0.11–0.36; Fig. 3a,c), and the correlations with the stability are also weak for the ERA5 long-term changes (r = 0.09–0.25; Fig. 4a). Figure 3a-b show that the largest LRF is collocated not with the strongest stability, but with the largest surface warming and oceanic heating. This is also true for the ERA5 long-term changes (Fig. 4). We found much stronger spatial correlations of LRF with surface warming (r = 0.97) and oceanic heating (r = 0.71) than LRF's correlations with stability (r = 0.11) over the Arctic Ocean in the 1%CO_2 run (Fig. 3a-b). In particular, over areas with the largest sea-ice loss, such as the Greenland Sea, Barents-Kara Seas (BKS) and the Bering Sea, oceanic heat release is largest (Fig. 3b) as sea-ice retreat exposes warm ocean water surfaces to heat the near-surface air directly. Such a surface-heating-induced warming weakens with height as it moves farther away from the heating source in the stable Arctic atmosphere, which prevents rapid vertical mixing through convection. This leads to large surface warming,

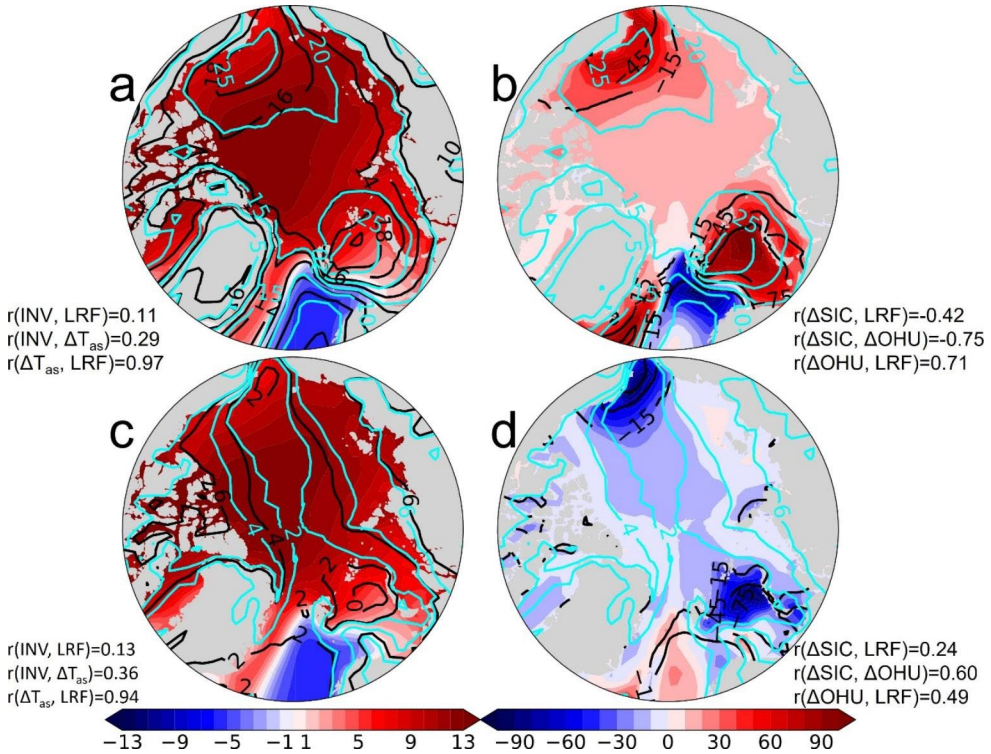

Fig. 3 (**a**, **c**) DJF temperature inversion (929 hPa minus surface air temperature difference; shading; in K; results are similar if potential temperature is used) averaged over years 1–80 of the CESM1 CTL run, and the change (years 131–150 relative to the CTL climatology) in surface air temperature (black contours; in K) and TOA radiative flux (positive downward) due to the lapse rate feedback (cyan contours; in W m^{-2}) for the (**a**) 1%CO_2 and (**c**) FixedIce runs. (**b**, **d**) DJF changes in oceanic heat uptake (shading; in W m^{-2}; positive upward), sea-ice concentration (black contours; in %; solid lines for negative values), and TOA radiative flux due to the lapse rate feedback (cyan contours; in W m^{-2}) for the (**b**) 1%CO_2 and (**d**) FixedIce runs. The pattern correlation between two fields is shown on the bottom corner of each panel. Each correlation coefficient has an associated *p*-value less than 0.01 and does not include land surfaces

strong vertical warming gradients, and large positive LRF over areas with large sea-ice loss (Figs. 2b and 3a-b). This is also true for the ERA5 long-term changes (Fig. 4), with the LRF's spatial correlation with surface warming, oceanic heating, and stability at 0.94, 0.82 and 0.09, respectively. The recent sea-ice loss also led to oceanic heat release of 15–90 W m^{-2} over the Greenland Sea, BKS and, to a lesser extent, over the Bering Sea (Fig. 4b). Further, without the oceanic heating (Fig. 3d), LRF is greatly reduced everywhere over the Arctic in FixedIce, despite the existence of the same strong inversion over most of the Arctic (Fig. 3c). With the oceanic heating of 20–90 W m^{-2} (Fig. 3b), which is large compared with the direct radiative forcing from the 4×CO_2 increase (which is about 7.4 W m^{-2}, Dai et al. 2020), large positive LRF is seen over many areas with weak or negative inversion (Fig. 3a). This suggests that strong stratification is not necessary for surface heating to generate a bottom-heavy warming profile in the Arctic, as long as the atmospheric is non-convective (i.e., without the strong vertical mixing through convection). These results suggest that it is the oceanic heat release caused by sea-ice loss that leads to enhanced surface warming and positive LRF in Arctic winter (when the atmosphere is stable and non-convective) under increasing CO_2. The results also suggest that without the effect of sea-ice loss, high stability together with all other processes can only produce a weak surface enhancement of CO_2-induced warming and thus weak positive LRF. Thus, sea-ice loss and the resultant oceanic heat release are a necessary condition for the occurrence of strong positive LRF in Arctic winter under increasing CO_2.

We notice that over the Norwegian Sea region, where relatively warm waters release large amounts of heat and moisture into the air and convection can occur in winter, both the inversion (Fig. 3a) and changes in ocean heat uptake (Fig. 3b) are negative, thus they cannot explain the weak but still positive LRF over this region (Fig. 3a). Similar weak positive LRF is also seen in FixedIce (Fig. 3c); thus, other processes besides the sea-ice loss-induced surface heating and stable stratification are likely behind the weak positive LRF over the Norwegian Sea region and in the FixedIce experiment. This also suggests that stable stratification or high stability, which is not the same as non-convective, is not a necessary condition for positive LRF to occur, in contrast to previous studies (e.g., Boeke et al. 2021).

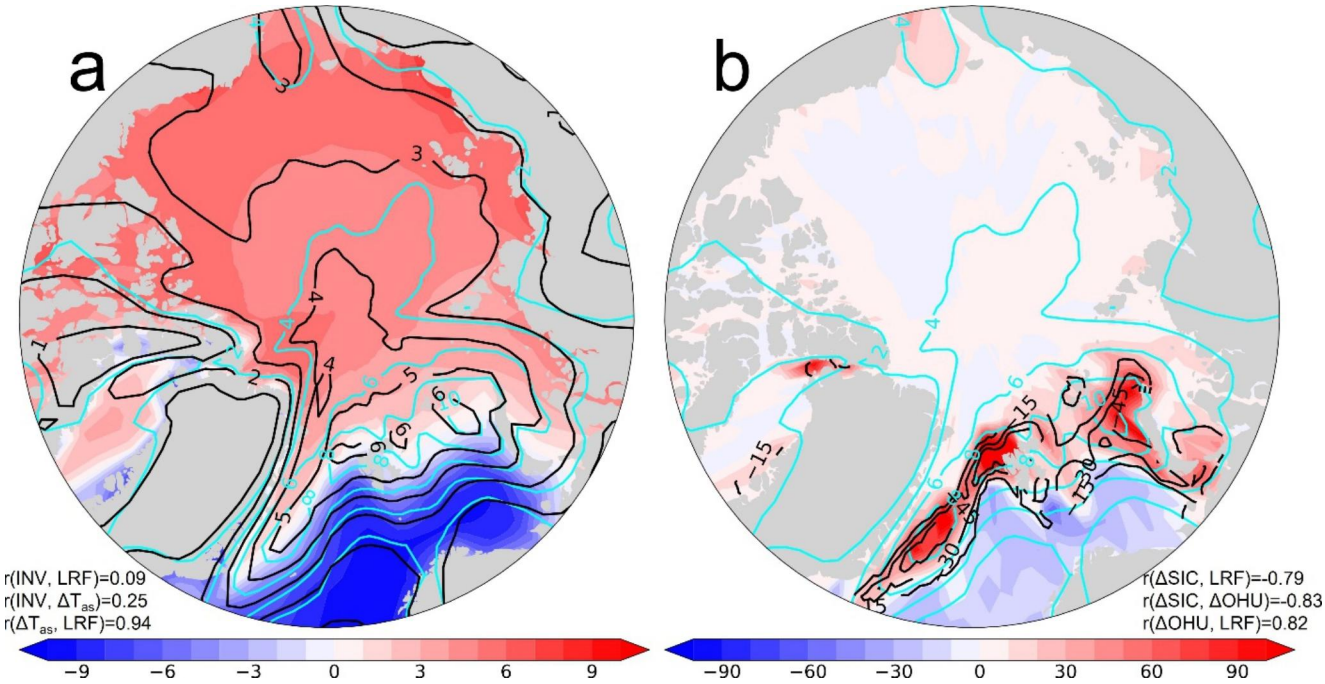

Fig. 4 (**a**) ERA5 DJF 1950–1979 mean temperature inversion (in K; shading; defined as $T_{850\,hPa} - T_{1000\,hPa}$), and changes (1990–2019 minus 1950–1979) in surface air temperature (in K; black contours) and TOA radiative flux due to the lapse rate feedback (in W m^{-2}; cyan contours). (**b**) ERA5 DJF changes (1990–2019 minus 1950–1979) in oceanic heat uptake (in W m^{-2}; shading; positive upward), sea-ice concentration (in %; black contours; solid lines for negative values), and TOA radiative flux (positive downward) due to the lapse rate feedback (in W m^{-2}; cyan contours). The pattern correlation between two fields is shown on the bottom corner of each panel. Each correlation coefficient has an associated *p*-value less than 0.01 and does not include land surfaces

Figure 5a shows that during DJF the positive LRF reduces the PLF roughly by 50%, leading to a net temperature feedback that is roughly half of the PLF in the 1%CO_2 run. This is also approximately true for ERA5 long-term changes; that is, the LRF cuts the PLF roughly by half, so that the net temperature feedback is only about half of the PLF. This illustrates an important role of the positive LRF in Arctic energy balance and surface warming in the fully coupled system when sea ice is allowed to respond to GHG-induced warming. To estimate the contribution of the LRF to surface warming, we calculated a hypothetic warming amount (shading in Fig. 6) that is vertically uniform and would result in the same TOA forcing as the net temperature feedback in the 1%CO_2 run or ERA5 through the Planck feedback only (i.e., without the LRF). The difference between the actual surface warming amount and this hypothetic warming amount (the black line in Fig. 6) represents the surface warming contribution by the LRF. Figure 6 shows that the LRF approximately doubles the DJF surface warming amount over most of the Arctic. Over areas with significant sea-ice loss, the LRF is slightly more effective in raising surface air temperature than over regions with little sea-ice loss in the 1%CO_2 run and ERA5 data (Fig. 6).

To investigate whether the increased cold-season oceanic heat release mainly comes from the increased oceanic absorption of solar radiation during the sunlit warm season, in Fig. 7 we compare the warm-season (May to August) integrated total net surface absorption of solar radiation (contours) and cold-season (September to April) integrated total net surface energy loss (shading) over the Arctic for both the current climatology (Fig. 7b) and their future changes (Fig. 7a). These specific months were chosen based on the mean annual cycle of the Arctic-mean surface net energy flux (see Suppl. Figure 1 in Dai et al. 2019). Figure 7 shows that the spatial patterns of both the climatology and future changes in the warm-season total absorption of solar radiation and cold-season total heat release are strongly correlated (r = 0.76–0.79) over the Arctic Ocean and the two are roughly in balance over the central Arctic (Fig. 7a-b), which suggests a strong relationship between the two. However, a closer look reveals that the large increase in the cold-season heat release over areas with large sea-ice loss, such as the BKS, Bering Sea, and Greenland Sea, greatly exceeds (by up to ~100%) the local increase in the warm-season solar absorption (Fig. 7a). This implies that there exists some horizontal redistribution or transport of heat within the upper ocean, which also occurs in the climatology over the Greenland Sea, Norwegian Sea, and BKS, where the cold-season heat release greatly exceeds the local warm-season absorption of solar radiation (Fig. 7b) likely due to

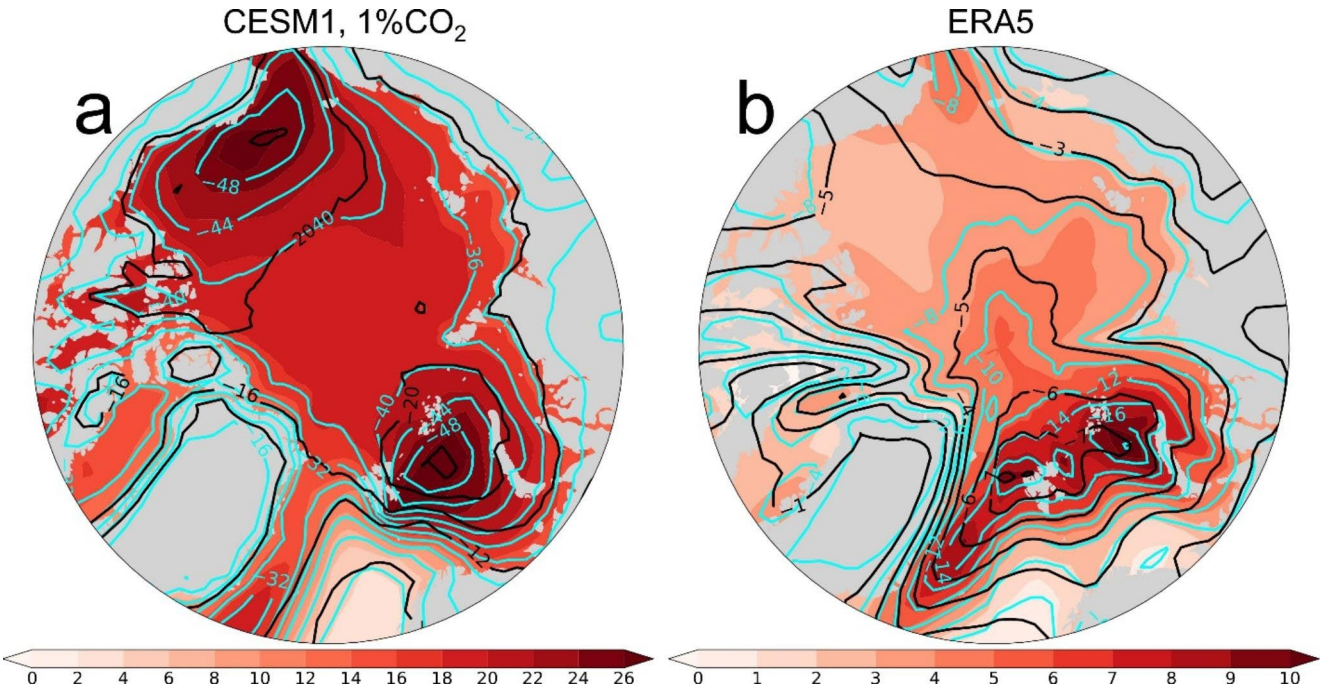

Fig. 5 (**a**) DJF TOA flux change (years 131–150 relative to the CTL climatology, positive downward, in W m^{-2}) in the CESM1 1%CO_2 run due to the lapse rate feedback (shading), Planck feedback (cyan contours), and total temperature feedback (black contours). (**b**) Same as (**a**), but for the ERA5 long-term changes from 1950–1979 to 1990–2019

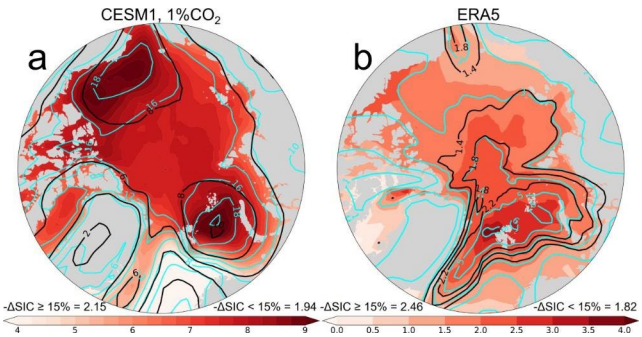

Fig. 6 (**a**) CESM1-simulated changes (years 131–150 relative to the CTL climatology) in DJF surface air temperature (in K) in the CESM1 1%CO_2 run without the effects of the lapse rate feedback (shading), with the effects of the LRF (cyan contours; in intervals of 2 K), and their difference (black contours; in intervals of 2 K). The hypothetic warming without the lapse rate feedback (shading) was calculated by assuming a vertically uniform warming profile that would result in the same TOA forcing as the net temperature feedback in the CESM1 1%CO_2 run. (**b**) Same as (**a**) but for the ERA5 long-term changes (1990–2019 minus 1950–1979). The ratios of the total warming to the warming without the LRF averaged over oceanic areas with 15% or more SIC loss or less than 15% SIC loss are shown on the bottom-left and bottom-right corners of each map, respectively

northward transport of heat by Atlantic Ocean circulation. Outside these regions, the two local fluxes match well in a climatological sense (Fig. 7b). Similar relationships are also seen for ERA5 long-term changes (Fig. 8); that is, the increase in the cold-season heat release greatly exceeds the increase in the warm-season absorption of solar radiation over areas with large sea-ice loss, even though the two local fluxes are roughly in balance in the climatology outside the North Atlantic subpolar region. These results suggest that the local increased warm-season absorption of solar radiation only provides a fraction of the increased cold-season heat release over areas with large sea-ice loss, even though the two are roughly in balance over the central Arctic Ocean where winter sea-ice loss is small. Horizontal heat transport within the oceans, including that from the North Atlantic (Mayer et al. 2019), plays an important role in the local energy balance within the Arctic Ocean.

Figure 9 compares the *potential* warming or cooling amounts that would be realized if the TOA forcing due to the individual feedbacks is used to generate a vertically-uniform equilibrium temperature change (or result from the temperature change) for the Arctic versus the globe for annual mean (Fig. 9a-b) and for Arctic winter versus summer (Fig. 9c-d) in the 1%CO_2 (Fig. 9a,c) and FixedIce (Fig. 9b,d) experiments. We emphasize that, except for the temperature feedbacks, these are not the actual warming or cooling amounts caused by the individual feedbacks since the TOA forcing may or may not be used to change the surface temperature in transient states, as explained in Sect. 2.3. Figure 9a shows that in the 1%CO_2 run, surface albedo and lapse-rate feedbacks have large positive (i.e., warming) contributions to Arctic warming whereas their contributions to

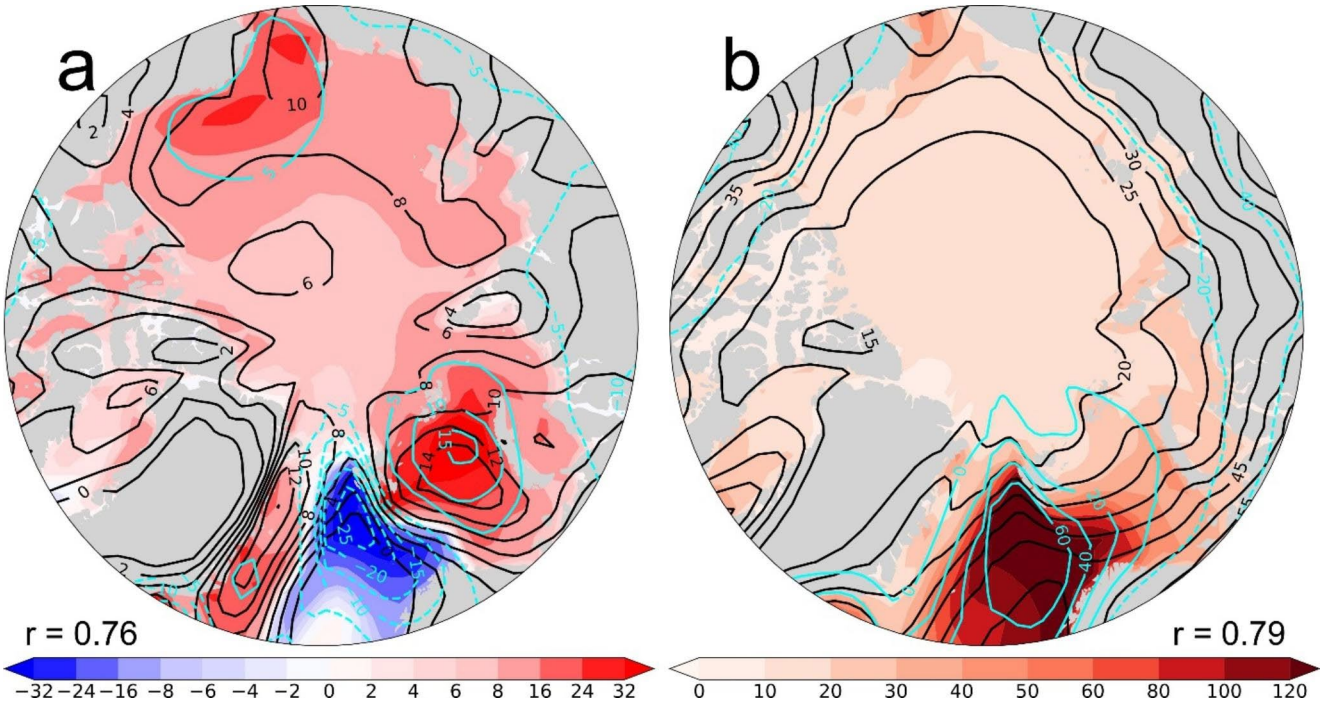

Fig. 7 (**a**) CESM1-simulated *changes* (relative to the CTL climatology) in the cold season (September-April) integrated net surface energy storage loss (shading; in MJ m^{-2}; positive upwards), warm-season (May-August) integrated net absorption of solar radiation (black contours; in MJ m^{-2}; positive downwards), and the shading-minus-black contour difference (cyan contours; in MJ m^{-2}) for years 131–150 of the 1%CO_2 run. (**b**) Similar to (**a**), except for the CTL *climatology* of the mean cold-season integrated net surface energy storage loss (shading; in MJ m^{-2}; positive upwards), mean warm-season integrated net absorption of solar radiation (black contours; in MJ m^{-2}; positive downwards), and their difference (cyan contours; in MJ m^{-2}) for years 1–80 of the CESM1 CTL run. The pattern correlation between the cold season and warm season integrated energy storage (over ocean only) is shown on the bottom corner of each panel. Each correlation coefficient has an associated *p*-value less than 0.01

global warming are small, thereby contributing to AA. Note the Planck and total temperature feedbacks are always negative, but their deviation from their global mean is positive for the Arctic, which means that they cause less cooing in the Arctic than for the globe and thus contribute positively to AA. The positive water vapor feedback is weaker in the Arctic than the globe, and cloud feedback is more negative in the Arctic than the globe, thus both contributing negatively to AA. These results generally agree with previous analyses of fully coupled model simulations, although the sign of the cloud feedback may differ among different models (e.g., Pithan and Mauritsen 2014; Feldl et al. 2020; Hahn et al. 2021). Figure 9 also shows that the ocean heat uptake change (ΔOHU) is a positive contributor to AA especially in winter (Fig. 9c), while atmospheric poleward heat transport change (ΔAPHT) contributes negatively to AA, as shown previously by Jenkins & Dai (2021) using DJF TOA fluxes. Figure 9c also shows that as ΔOHU becomes downward (i.e., increased oceanic absorption of solar radiation) in summer, the warming contribution by LRF becomes negligible; while LRF greatly contributes to Arctic warming (by ~5.0 K, the largest of all processes) in winter when ΔOHU is upward (i.e., oceanic heating due to sea-ice loss). This suggests that oceanic heating of the air is important for the occurrence of the large positive LRF in the Arctic.

When the effect of sea-ice loss is absent, all Arctic climate feedbacks become much weaker than in the fully coupled 1%CO_2 run except for water vapor feedback, which weakens only slightly; while ΔOHU becomes negative (i.e., downward and thus negative contributions to atmospheric warming) and ΔAPHT becomes northward (i.e., positive contribution to Arctic warming) (Fig. 9b). In particular, the winter potential warming contribution by LRF decreases from ~5.0 K in the 1%CO_2 run to ~1.25 K in FixedIce, as the winter ΔOHU changes from a warming contribution of ~2.6 K in the 1%CO_2 run to a cooling contribution of -1.6 K in FixedIce (Fig. 9c,d). This further shows that significant oceanic heating is necessary for the occurrence of large positive LRF in the Arctic. Because of the lack of oceanic heating and weakened feedbacks, the AA and Arctic warming are also much weaker in FixedIce (Table 1; Fig. 3a,c). These results suggest that most Arctic climate feedbacks, including Arctic lapse-rate, cloud, surface albedo, temperature and Planck feedbacks, would weaken greatly without increased oceanic heat release from sea-ice loss, which could happen during the 23rd century when most Arctic sea ice is gone

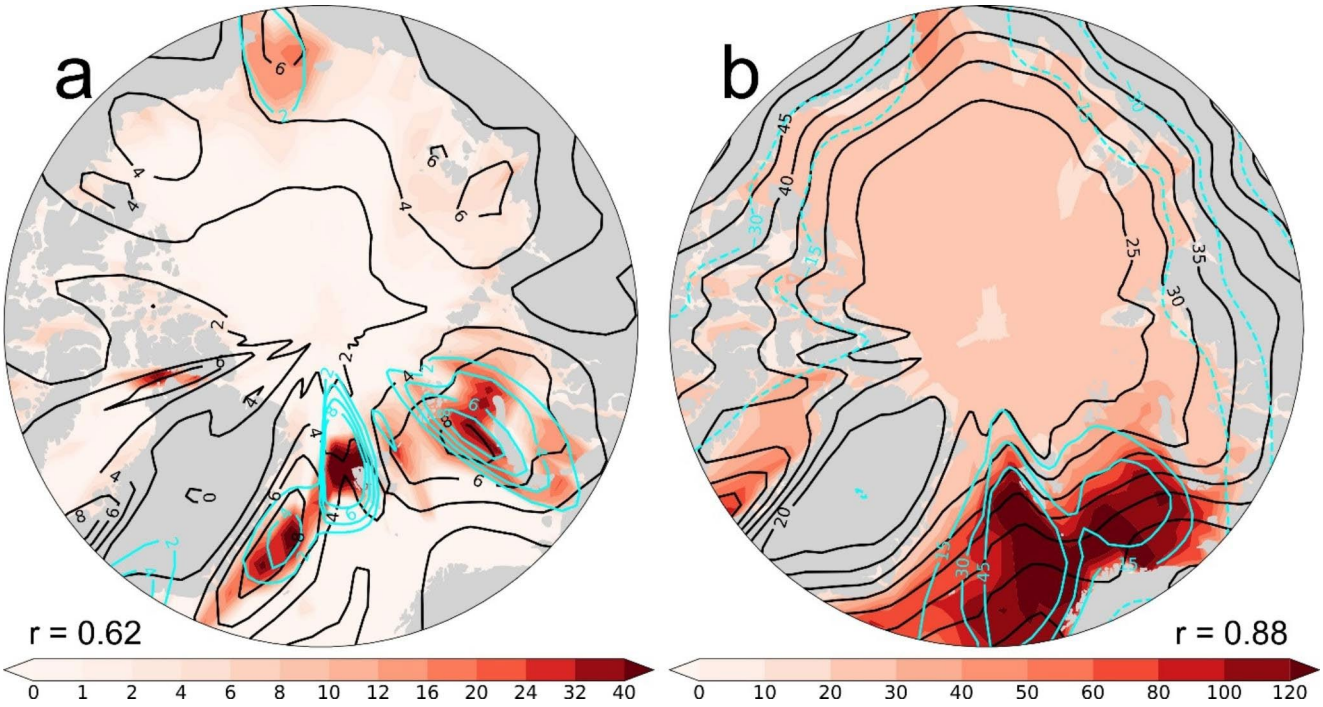

Fig. 8 (**a**) ERA5 long-term *changes* (years 1990–2019 minus years 1950–1979) in the cold-season (September-April) integrated net surface energy storage loss (shading; in MJ m^{-2}) and warm-season (May-August) integrated net shortwave (SW) energy storage gain (contours, in MJ m^{-2}). (**b**) Similar to (**a**), except for the climatology of the cold-season loss and warm-season gain averaged over years 1950–1979. The cyan contours represent the difference between the cold season integrated net energy storage loss and warm season integrated net energy storage gain. The pattern correlation between the cold season and warm season integrated energy storage (over ocean only) is shown on the bottom corner of each panel. Each correlation coefficient has an associated *p*-value less than 0.01 and does not include land surfaces

even during winter (Dai et al. 2019). This illustrates the crucial role of sea-ice loss: the strength of Arctic climate feedbacks, Arctic warming and AA greatly depends on Arctic sea-ice loss and the resultant heating from the ocean. The winter oceanic heating induced by sea-ice loss can not only directly cause significant surface warming (Fig. 9c), but also lead to stronger lapse-rate and other positive feedbacks, thereby further contributing to AA.

Most of the Arctic climate feedbacks are stronger in winter than in summer, except for surface albedo and water vapor feedbacks, which are stronger in summer (Fig. 9c). This is consistent with the stronger oceanic heat release due to sea-ice loss in winter (Fig. 9c; Dai et al. 2019; Jenkins and Dai 2021), which can amplify the Arctic climate feedbacks as noticed above. When the effect of sea-ice loss is suppressed, most of the winter Arctic climate feedbacks, as well as summer cloud and albedo feedbacks, weaken (Fig. 9d). Figure 9 shows that Arctic cloud feedback is very sensitive to sea-ice loss and the resultant oceanic heating and surface warming for annual, DJF and JJA: sea-ice loss leads to stronger negative cloud feedback in the Arctic in summer and for annual mean, but slightly enhance the positive cloud feedback in winter (Fig. 9).

Figure 10 shows that ERA5 long-term changes qualitatively show similar warming/cooling contributions by the feedbacks, ΔOHU and ΔAPHT, except for Arctic cloud feedback, which is negative in CESM1 1%CO_2 run (mainly in summer, Fig. 9a,c) but positive for the ERA5 long-term change (mainly in winter). That is, the winter cloud feedback is positive in both CESM1 and ERA5, but summer cloud feedback is strongly negative in CESM1 but only slightly negative in ERA5. Thus, the cloud feedback difference comes mainly from summer. Similar to CESM1 (except for the cloud feedback), ERA5 also shows stronger Arctic climate feedbacks in winter than in summer, except the surface albedo feedback which occurs mainly in the sunlit warm season (Fig. 10b). Thus, except for summer cloud feedback, Arctic climate feedbacks and their seasonality in CESM1 are qualitatively consistent with those based on ERA5 long-term changes from 1950 to 1979 to 1990–2019.

4 Summary and discussion

To examine the relationships among Arctic warming, LRF, stability, sea-ice loss and oceanic heat release, we analyzed the changes around the time of 4×CO_2 in two CESM1 simulations both with 1%/year CO_2 increases, one with fully coupled sea ice (1%CO_2) and another with fixed sea-ice cover (FixedIce) in calculating surface fluxes. For comparison, we

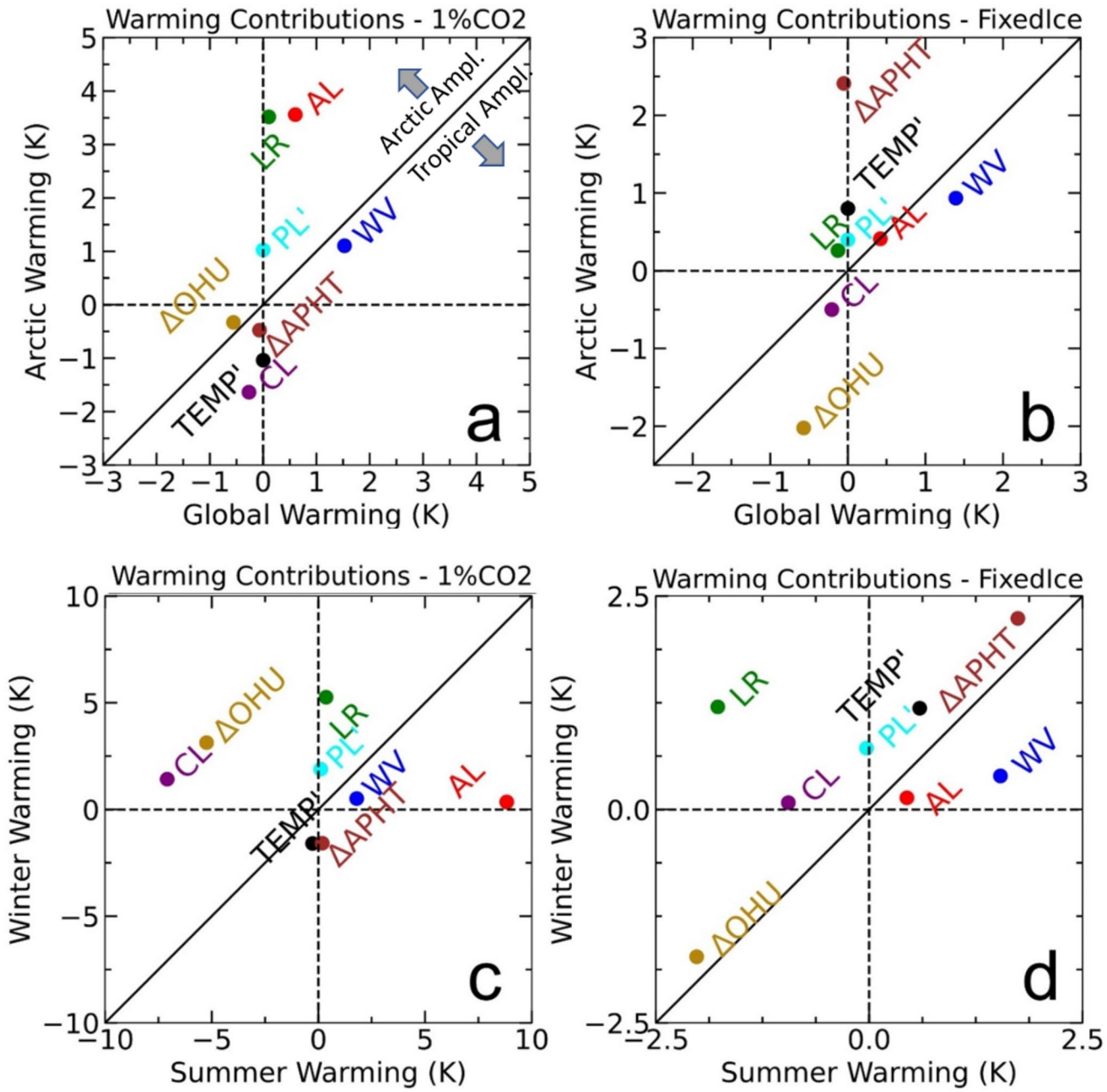

Fig. 9 (**a**, **b**) Arctic (67°–90°N) vs. global annual *potential* warming contributions (in K) from surface albedo (AL), water vapor (WV), cloud (CL) and lapse rate (LR) feedbacks, changes in atmospheric poleward heat transport (ΔAPHT) and oceanic heat uptake (ΔOHU, positive upward), and the deviation from the global mean of the Arctic Planck (PL′ = Arctic PL – global-mean PL) and temperature (TEMP′ = Arctic TEMP – global-mean TEMP) feedbacks for the CESM1 (**a**) 1%CO_2 and (**b**) FixedIce runs around the time of 4×CO_2. A process above (below) the diagonal line in (**a, b**) represents a positive (negative) contribution to Arctic amplification. (**c**, **d**) Similar to (**a**) and (**b**), but for the Arctic winter (December-January-February) vs. summer (June-July-August) *potential* warming contributions. Note the different x- and y-axis scales used in (**a-d**). The global-mean Planck feedback contribution is -4.02 (-3.39) K for the 1%CO_2 (FixedIce) run. The global-mean temperature feedback contribution is -3.91 (-3.55) W m^{-2} K^{-1} for the 1%CO_2 (FixedIce) run

also analyzed long-term changes from 1950–1979 to 1990–2019 in ERA5 data. Results show that Arctic positive LRF is a result of the enhanced surface warming relative to free-tropospheric warming in winter, and this surface warming enhancement results mainly from increased oceanic heating of the air due to sea-ice loss, while the degree of atmospheric stability plays a minor role. We found that without the oceanic heating induced by sea-ice loss, all other processes cannot generate a strong bottom-heavy warming profile and large positive LRF in stable Arctic air, and

Table 1 December-January-February mean surface warming (in K) with the effects of the LRF (ΔT_{as}) and without the effects of the LRF (ΔT_{as} w/o LRF) for the 1%CO_2 and FixedIce runs, and ERA5 data averaged over the Arctic region (67°-90°N), the globe, and the Arctic to global mean surface warming ratio (i.e., Arctic amplification or AA).

	1%CO_2			ERA5			FixedIce		
	Arctic	Global	AA	Arctic	Global	AA	Arctic	Global	AA
ΔT_{as}(K)	14.18	3.60	3.94	3.33	0.45	7.37	3.63	2.85	1.27
ΔT_{as}w/o LRF (K)	7.10	3.65	1.95	1.73	0.51	3.41	2.54	3.26	0.78

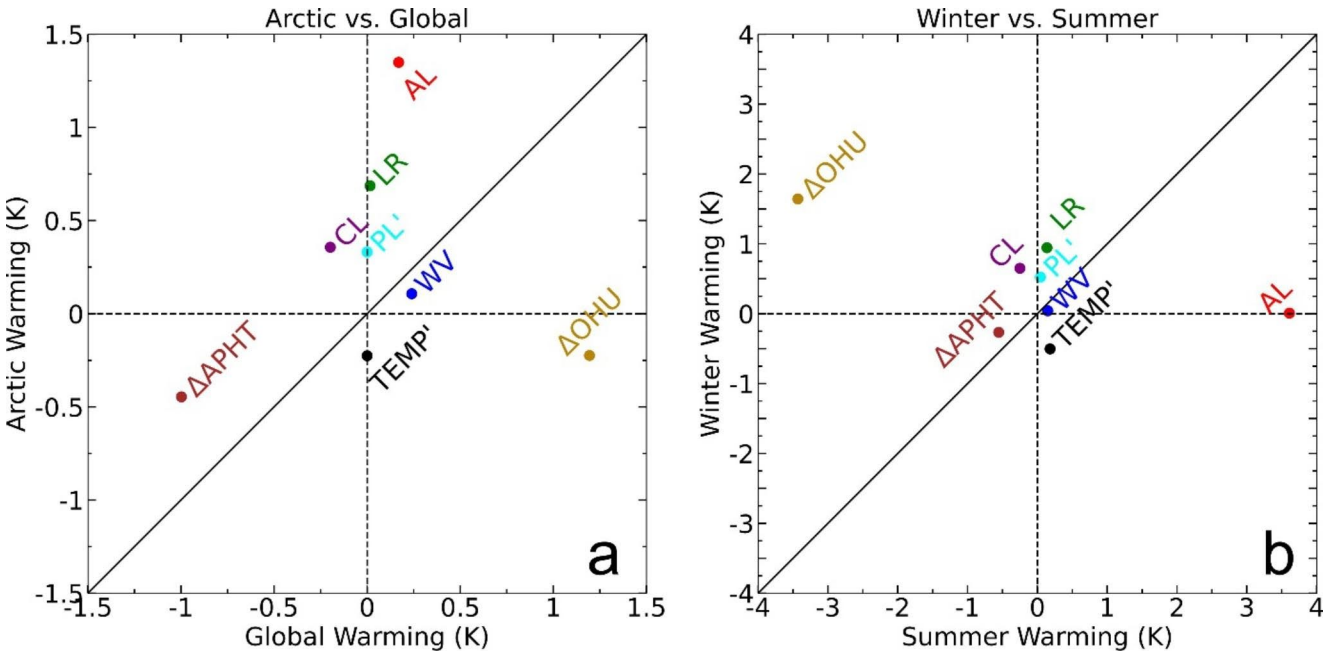

Fig. 10 Similar to Fig. 9 but based on the long-term changes (1990–2019 minus 1950–1979) in ERA5 data for (**a**) annual Arctic (67°-90°N) vs. global and (**b**) Arctic winter (December-January-February) vs. summer (June-July-August) feedback warming contributions (in K). The global-mean PL and TEMP feedback contributions are − 0.61 K and − 0.60 K, respectively

strong atmospheric stability is unnecessary for the surface heating to generate large positive LRF in Arctic non-convective environment. Further, we showed that most Arctic climate feedbacks (including LRF), except for water vapor feedback, weaken greatly when the oceanic heating induced by sea-ice loss is absent, leading to greatly reduced Arctic warming and AA as seen in our FixedIce experiment. Thus, sea-ice loss and the resultant oceanic heat release in winter not only directly warm the near-surface air and the lower troposphere, but also greatly enhance Arctic lapse-rate and other feedbacks, further contributing to Arctic surface warming and AA.

The winter oceanic heating induced by sea-ice loss is efficient in raising surface air temperature without causing large upper-level warming in a non-convective environment like the Arctic, producing large positive LRF; while all other processes tend to produce similar warming near the surface and in the troposphere, leading to a weak positive LRF despite the existence of strong stability, as shown in our FixedIce experiment. This is not surprising given that an upward surface heating is expected to warm the surface air first, while all downward heating will warm both the troposphere and the surface simultaneously. With the existence of the bottom-heavy warming profile, the strong positive LRF allows the oceanic heat release to raise surface air temperature more effectively. Our calculations indicate that the LRF roughly doubles the warming compared with the case without the LRF under the same Arctic energy balance. Thus, while the large positive LRF results mainly from sea-ice loss and the resultant oceanic heat release, its existence greatly enhances Arctic surface warming under rising atmospheric CO_2.

We also found that the increase in cold-season oceanic heat release greatly exceeds the increase in local warm-season absorption of solar radiation over areas with large sea-ice loss, even though they are roughly in balance on a climatological sense over most of the Arctic (except for the Greenland Sea, Norwegian Sea and BKS). This indicates that local increased solar absorption can only provide a fraction of the increased winter heat release over areas with sea-ice loss, suggesting a redistribution or transport of energy within the upper ocean between the two seasons.

The weak relationship between Arctic LRF and atmospheric stability, and the large warming effect of the oceanic heating induced by sea-ice loss revealed by our CESM1 experiments are consistent with our analysis of the long-term changes in ERA5 data, as well as those done by Jenkins and Dai (2022). It is also in agreement with Feldl et al. (2020) and Boeke et al. (2021), who showed that Arctic LRF is dictated by surface warming patterns rather than the degree of atmospheric stability among climate models, and the surface warming pattern or amount is not closely tied to atmospheric stability. In particular, Feldl et al. (2020) concluded that positive LRF in high latitudes arises primarily from sea-ice loss and atmospheric circulation changes. Feldl et al. (2020) emphasized the role of Arctic ice-albedo feedback (through its delayed impact on winter surface fluxes), which can only account for a fraction of the increased cold-season oceanic heat release over areas with large sea-ice loss (Figs. 7 and 8). In contrast, here we showed that the increased winter oceanic heat release after sea-ice retreat is the main cause of the enhanced Arctic surface warming and the resultant positive LRF, rather than the summer increased absorption of solar radiation or changes in atmospheric energy transport.

Our weak LRF in FixedIce is also consistent with Graversen et al. (2014), who found that LRF accounts for only 15% of the AA in a climate model without the impacts of sea-ice loss on surface fluxes, and the LRF is closely coupled to other processes. However, our results are inconsistent with the conventional notion that Arctic high stability confines GHG-induced warming near the surface and is largely responsible for the amplified surface warming in the Arctic (Manabe and Wetherald 1975; Hansen et al. 1984; Bintanja et al. 2011) and thus Arctic positive LRF.

While recent studies (e.g., Feldl et al. 2020; Boeke et al. 2021) have shown a strong relationship between Arctic LRF and surface warming patterns and Feldl et al. (2020) indicated a key role of sea-ice loss in generating Arctic positive LRF, our results further demonstrate that *winter* sea-ice loss and the resultant oceanic heat release are a necessary condition for large positive LRF to occur in the Arctic non-convective air, while strong stratification is unnecessary for the oceanic heating to generate large positive LRF. Further, we have identified the specific key physical process (namely the winter oceanic heat release after sea-ice retreat) that is largely responsible for the enhanced surface warming that leads to the large positive LRF, and quantified the contribution by the LRF to Arctic warming under rising CO_2. We also showed that most Arctic climate feedbacks, except the water vapor feedback, would weaken greatly if the sea-ice loss-induced heating is absent. These are new findings not addressed previously.

Our findings have major implications for future climate when Arctic sea ice could melt away during many of the cold-season months by the 23rd century (Dai et al. 2019). If that were to happen, Arctic LRF would become weak together with weak additional Arctic amplification (Dai et al. 2019). Thus, the existence of sea ice has major impacts on Arctic climate response to increasing GHGs, including Arctic lapse-rate and other feedbacks.

We conclude that the enhanced surface warming in the Arctic (and thus the AA) results primarily from increased oceanic heating in the cold season due to sea-ice loss, while high stability only plays a minor role. The enhanced surface warming (relative to upper levels) leads to large Arctic positive LRF, which roughly doubles Arctic warming under rising GHGs. Without the oceanic heating induced by sea-ice loss, most Arctic climate feedbacks (including LRF) would weaken greatly, leading to reduced Arctic warming and weak AA. Snow-ice albedo feedback over high latitude land could also enhance warming; however, Dai et al. (2019) showed that without large winter sea-ice loss, all other processes can only produce weak AA.

Author contributions A. Dai designed the study, helped formulate the data analysis and design of the figures, wrote the manuscript; M. Jenkins helped design the study, made all the figures and helped improve the manuscript.

Funding This work was funded by University at Albany of SUNY and NSF (Grants AGS-2015780 and OISE-1743738).

Data Availability The CESM1 model data used here are available from https://doi.org/10.4121/14699514. ERA5 data are available from https://www.ecmwf.int/en/forecasts/datasets/reanalysis-datasets/era5.

Declarations

Ethics approval Not applicable.

Consent for publication The authors agree to publish the paper in *Climate Dynamics*.

Competing interests None.

References

Barnes EA, Polvani LM (2015) CMIP5 projections of Arctic amplification, of the North American/North Atlantic circulation, and of their relationship. J Clim 28:5254–5271. https://doi.org/10.1175/JCLI-D-14-00589.1

Bintanja R, Graversen RG, Hazeleger W (2011) Arctic winter warming amplified by the thermal inversion and consequent low infrared cooling to space. Nat Geosci 4:758–761. https://doi.org/10.1038/ngeo1285

Boeke RC, Taylor PC (2018) Seasonal energy exchange in sea ice retreat regions contributes to differences in projected Arctic warming. Nat Comm 9:5017. https://doi.org/10.1038/s41467-018-07061-9

Boeke RC, Taylor PC, Sejas SA (2021) On the nature of the Arctic's positive lapse-rate feedback. Geophys Res Lett 48:e2020GL091109. https://doi.org/10.1029/2020GL091109

Burt MA, Randall DA, Branson MD (2016) Dark warming. J Clim 29:705–719

Cai M (2005) Dynamical amplification of polar warming. Geophys Res Lett 32:L22710. https://doi.org/10.1029/2005GL024481

Chung E-S, Ha K-J, Timmermann A, Stuecker MF, Bodai T, Lee S-K (2021) Cold-season Arctic amplification driven by Arctic ocean-mediated seasonal energy transfer. *Earth's Future*, *9*, e2020EF001898. https://doi.org/10.1029/2020EF001898

Dai A (2022) Arctic amplification is the main cause of the Atlantic meridional overturning circulation weakening under large CO_2 increases. Clim Dyn 58:3243–3259. https://doi.org/10.1007/s00382-021-06096-x

Dai A, Deng J (2021) Arctic amplification weakens the variability of daily temperatures over northern middle-high latitudes. J Clim 34:2591–2609

Dai A, Song M (2020) Little influence of Arctic amplification on midlatitude climate. Nat Clim Chang 10:231–237. https://doi.org/10.1038/s41558-020-0694-3

Dai A, Wigley TML, Boville BA, Kiehl JT, Buja LE (2001) Climates of the 20th and 21st centuries simulated by the NCAR Climate System Model. J Clim 14:485–519

Dai A, Luo D, Song M, Liu J (2019) Arctic amplification is caused by sea-ice loss under increasing CO_2. Nat Comm 10:121. https://doi.org/10.1038/s41467-018-07954-9

Dai A, Huang D, Rose BEJ, Zhu J, Tian X (2020) Improved methods for estimating equilibrium climate sensitivity from transient warming simulations. Clim Dyn 54:4515–4543. https://doi.org/10.1007/s00382-020-05242-1

Deng J, Dai A (2022) Sea ice-air interactions amplify multidecadal variability in the North Atlantic and Arctic region. Nat Commun 13:2100. https://www.nature.com/articles/s41467-022-29810-7

Deser C, Tomas R, Alexander M, Lawrence D (2010) The seasonal atmospheric response to projected Arctic sea ice loss in the late twenty-first century. J Clim 23:333–351. https://doi.org/10.1175/2009JCLI3053.1

England MR, Eisenman I, Lutsko NJ, Wagner TJW (2021) The recent emergence of Arctic amplification. Geophys. Res. Lett, 48, e2021GL094086. https://doi.org/10.1029/2021GL094086

Feldl N, Po-Chedley S, Singh HKA, Hay S, Kushner PJ (2020) Sea ice and atmospheric circulation shape the high-latitude lapse rate feedback. Clim Atmos Sci 3:41. https://doi.org/10.1038/s41612-020-00146-7

Gong T, Feldstein S, Lee S (2017) The role of downward infrared radiation in the recent Arctic winter warming trend. J Clim 30:4937–4949. https://doi.org/10.1175/JCLI-D-16-0180.1

Goosse H, Kay JE, Armour KC, Bodas-Salcedo A, Chepfer H, Docquier D et al (2018) Quantifying climate feedbacks in polar regions. *Nature Comm*, *9*, 1919. https://doi.org/10.1038/s41467-018-04173-0

Graham RM, Cohen L, Ritzhaupt N, Segger B, Graverson RG, Rinke A et al (2019) Evaluation of six atmospheric reanalyses over Arctic sea ice from winter to early summer. J Clim 32:4121–4143

Graversen RG, Langen PL, Mauritsen T (2014) Polar amplification in CCSM4: contributions from the lapse rate and surface albedo feedbacks. J Clim 27:4433–4450. https://doi.org/10.1175/JCLI-D-13-00551.1

Hahn LC, Armour KC, Zelinka MD, Bitz CM, Donohue A (2021) Contribution to polar amplification in CMIP5 and CMIP6 models. Front Earth Sci 9:710036. https://doi.org/10.1175/JCLI-D-21-0626.1

Hansen JE, Lacis A, Rind D, Russell G, Stone P, Fung I et al (1984) Climate sensitivity: analysis of feedback mechanisms. Clim Processes Clim Sensit Geophysical Monograph 29:130–163

Hersbach H, Bell B, Berrisford P, Hirahara S, Horányi A, Muñoz-Sabater J et al (2020) The ERA5 global reanalysis. Q J Royal Meteorol Soc 146:1999–2049. https://doi.org/10.1002/qj.3803

Hirahara S, Balmaseda MA, de Boisseson E, Hersbach H (2016) Sea surface temperature and sea ice concentration for ERA5. ERA Report Series No. 26, 25pp. Available at https://www.ecmwf.int/file/46880/download?token=4pKnkudy

Huang Y, Xia Y, Tan X (2017) On the pattern of CO2 radiative forcing and poleward energy transport. J Geophys Research: Atmos 122(20):10578–10593. https://doi.org/10.1002/2017JD027221

Hurrell JW, Holland MM, Gent PR, Ghan S, Kay JE, Kushner PJ et al (2013) The Community Earth System Model: a framework for collaborative research. Bull Amer Meteor Soc 94:1339–1360. https://doi.org/10.1175/BAMS-D-12-00121.1

Jenkins M, Dai A (2021) The impact of sea-ice loss on Arctic climate feedbacks and their role for Arctic amplification. Geophys Res Lett 48:e2021GL094599. https://doi.org/10.1029/2021GL094599

Jenkins MT, Dai A (2022) Arctic climate feedbacks in ERA5 reanalysis: Seasonal and spatial variations and the impact of sea-ice loss. Geophys Res Lett 49:e2022GL099263. https://doi.org/10.1029/2022GL099263

Jenkins MT, Dai A, Deser C (2023) Seasonal variations and spatial patterns of Arctic cloud changes in association with sea-ice loss during 1950–2019 in ERA5. *J. Climate*, submitted

Kay JE, Gettelman A (2009) Cloud influence on and response to seasonal Arctic sea ice loss. J Geophys Res 114:D18204. https://doi.org/10.1029/2009JD011773

Kumar A, Perlwitz J, Eischeid J, Quan X, Xu T, Zhang T et al (2010) Contribution of sea ice loss to Arctic amplification. Geophys Res Lett 37:L21701. https://doi.org/10.1029/2010GL045022

Lawrence H, Bormann N, Sandu I, Day J, Farnan J, Bauer P (2019) Use and impact of Arctic observations in the ECMWF numerical weather prediction system. Q J Royal Meteorol Soc 145:3432–3454

Manabe S, Wetherald RT (1975) The effects of doubling the CO_2 concentration on the climate of a general circulation model. J Atmos Sci 32:3–15. https://doi.org/10.1175/1520-0469(1975)032%3C0003:TEODTC%3E2.0.CO;2

Mayer M, Teitsche S, Haimberger L, Tsubouchi T, Mayer J, Zuo H (2019) An improved estimate of the coupled Arctic energy budget. J Clim 32:7915–7934. https://doi.org/10.1175/JCLI-D-19-0233.1

Miyawaki O, Tan Z, Shaw TA, Jansen MF (2020) Quantifying key mechanisms that contribute to the deviation of the tropical warming profile from a moist adiabat. *Geophys. Res. Lett. 47*, e2020GL089136. https://doi.org/10.1029/2020GL089136

Pendergrass AG, Conley A, Vitt FM (2018) Surface and top-of-atmosphere radiative feedback kernels for CESM-CAM5. Earth Syst Sci Data 10:317–324. https://doi.org/10.5194/essd-10-317-2018

Pithan F, Mauritsen T (2014) Arctic amplification dominated by temperature feedbacks in contemporary climate models. Nat Geosci 7:181–184. https://doi.org/10.1038/NGEO2071

Previdi M, Janoski TP, Chiodo G, Smith KL, Polvani LM (2020) Arctic amplification: a rapid response to radiative forcing. Geophys Res Lett 47:e2020GL089933. https://doi.org/10.1029/2020GL089933

Previdi M, Smith KL, Polvani LM (2021) Arctic amplification of climate change: a review of underlying mechanisms. Environ Res Lett 16:093003. https://doi.org/10.1088/1748-9326/ac1c29

Renfrew IA, Barrell C, Elvidge AD, Brooke JK, Duscha C, King JC et al (2021) An evaluation of surface meteorology and fluxes over the Iceland and Greenland Seas in ERA5 reanalysis: the impact of sea ice distribution. Q J Royal Meteorol Soc 147:691–712

Screen JA, Simmonds I (2010a) The central role of diminishing sea ice in recent Arctic temperature amplification. Nature 464:1334–1337

Screen JA, Simmonds I (2010b) Increasing fall-winter energy loss from the Arctic Ocean and its role in Arctic

temperature amplification. Geophys Res Lett 37:L16707. https://doi.org/10.1029/2010GL044136
Serreze MC, Francis JA (2006) The Arctic amplification debate. Clim Change 76:241–264
Serreze MC, Barrett AP, Stroeve JC, Kindig DM, Holland MM (2009) The emergence of surface-based Arctic amplification. *Cryosphere 3*, 11–19
Soden BJ, Held IM, Colman R, Shell KM, Kiehl JT, Shields CA (2008) Quantifying climate feedbacks using radiative kernels. J Clim 21:3504–3520. https://doi.org/10.1175/2007JCLI2110.1
Soldatenko S (2021) Effects of global warming on the poleward heat transport by non-stationary large-scale atmospheric eddies, and feedbacks affecting the formation of the Arctic climate. J Mar Sci Eng 9:867. https://doi.org/10.3390/jmse9080867
Stuecker MF, Bitz CM, Armour KC, Proistosescu C, Kang SM, Xie S-P et al (2018) Polar amplification dominated by local forcing and feedbacks. Nat Clim Chang 8:1076–1081. https://doi.org/10.1038/s41558-018-0339-y
Taylor PC, Boeke RC, Boisvert LN, Feldl N, Henry M, Huang Y et al (2022) Process drivers, inter-model spread, and the path forward: a review of amplified Arctic warming. Front Earth Sci 9:758361. https://doi.org/10.3389/feart.2021.758361
Wang Y, Huang Y (2021) A single-column simulation-based decomposition of the tropical upper-tropospheric warming. J Clim 34:5337–5348. https://doi.org/10.1175/JCLI-D-20-0726.1
Wang C, Graham RM, Wang K, Gerland S, Granskog MA (2019) Comparison of ERA5 and ERA-interim near surface air temperature, snowfall and precipitation over Arctic Sea ice: effects on sea ice thermodynamics and evolution. The Cryosphere 13:1661–1679
Yeo H, Kim M-H, Son S-W, Jeong J-H, Yoon J-H, Kim B-M et al (2022) Arctic cloud properties and associated radiative effects in three newer reanalysis datasets (ERA5, MERRA-2, JRA-55): discrepancies and possible causes. Atmos Res 270:106080